Muon spin relaxation evidence for the U(1) quantum spin-liquid ground state in the triangular antiferromagnet YbMgGaO4

Yuesheng Li, Devashibhai Adroja, Pabitra K. Biswas, Peter J. Baker, Qian Zhang, Juanjuan Liu, Alexander A. Tsirlin, Philipp Gegenwart, Qingming Zhang

Muon Spin Relaxation Evidence for the U(1) Quantum Spin-Liquid Ground State in the Triangular Antiferromagnet YbMgGaO₄

Yuesheng Li,[1,2,*] Devashibhai Adroja,[3,4] Pabitra K. Biswas,[3] Peter J. Baker,[3] Qian Zhang,[1] Juanjuan Liu,[1]
Alexander A. Tsirlin,[2] Philipp Gegenwart,[2] and Qingming Zhang[1,5,†]

[1]*Department of Physics, Renmin University of China, Beijing 100872, People's Republic of China*
[2]*Experimental Physics VI, Center for Electronic Correlations and Magnetism, University of Augsburg, 86159 Augsburg, Germany*
[3]*ISIS Pulsed Neutron and Muon Source, STFC Rutherford Appleton Laboratory,
Harwell Campus, Didcot, Oxfordshire OX11 0QX, United Kingdom*
[4]*Highly Correlated Matter Research Group, Physics Department, University of Johannesburg,
P.O. Box 524, Auckland Park 2006, South Africa*
[5]*Collaborative Innovation Center of Advanced Microstructures, Nanjing 210093, People's Republic of China*

Muon spin relaxation (μSR) experiments on single crystals of the structurally perfect triangular antiferromagnet YbMgGaO₄ indicate the absence of both static long-range magnetic order and spin freezing down to 0.048 K in a zero field. Below 0.4 K, the μ^+ spin relaxation rates, which are proportional to the dynamic correlation function of the Yb^{3+} spins, exhibit temperature-independent plateaus. All these μSR results unequivocally support the formation of a gapless U(1) quantum spin liquid ground state in the triangular antiferromagnet YbMgGaO₄.

Introduction.—Antiferromagnetically coupled ($J > 0$) spins on a perfect geometrically frustrated lattice, such as the triangular or kagome lattices, can preserve strong fluctuations and evade long-range order or spin freezing even at $T \ll J$. They reveal exotic phases characterized by interesting properties, such as fractionalized spin excitations, intrinsic topological order, and gapless excitations without symmetry breaking. These new phases have been proposed as quantum spin liquids (QSLs) [1–3]. The spin-$\frac{1}{2}$ triangular Heisenberg antiferromagnet, initially believed to host a resonating-valence-bond QSL ground state (GS) [4–6], develops, in fact, the 120°-type magnetic order [7–11]. However, this order is very fragile and can be melted by perturbations, such as next-nearest-neighbor couplings [12,13], spatially anisotropic interactions [14–16], and bond randomness [17]. Theoretical studies found that ring couplings destroy long-range order as well and trigger the formation of a U(1) QSL GS with a spinon Fermi surface [18–20]. On the other hand, relevant experimental systems, κ-(BEDT-TTF)₂Cu₂(CN)₃ [21] and EtMe₃Sb[Pd(dmit)₂]₂ [22], revealed linear temperature dependence of the heat capacity, in contrast to $C_v \sim T^{2/3}$ predicted for the U(1) QSL [18].

Recently, our group reported a new structurally perfect rare-earth triangular antiferromagnet YbMgGaO₄ [23,24]. Unlike the majority of QSL candidates, YbMgGaO₄ is free from magnetic defects [25–29], spatial anisotropy [29–31], and antisymmetric Dzyaloshinsky-Moriya anisotropy [32,33]. Its magnetic heat capacity reveals the $C_v \sim T^{2/3}$ behavior with almost zero residual entropy down to ∼0.06 K [23] compatible with the triangular U(1) QSL GS [18].

The spin susceptibility of a U(1) QSL is expected to approach a constant value as the temperature goes down to zero [18–20]. While the divergent nature of the bulk static susceptibility of YbMgGaO₄ was measured down to 0.48 K [23], this experimental temperature range was certainly not low enough to probe GS properties in a system, where J_0 is as low as 1.5 K [24]. In the following, we fill this gap by probing YbMgGaO₄ down to 0.048 K and provide evidence for the U(1) QSL GS.

Weak magnetic couplings between the rare-earth Yb^{3+} spins render the experimental probe of the GS extremely challenging. While nuclear magnetic resonance requires an external field on the order of 1 T that inevitably perturbs such a system, inelastic neutron scattering can be performed in a zero field, but fails to detect an inelastic signal at transfer energies below 0.1 meV, owing to the contamination by the elastic signal. In this respect, muon spin relaxation (μSR) is an ideal technique that can be performed in a true zero field (ZF). ZF-μSR is an extremely sensitive probe detecting tiny internal fields on the order of 0.1 G. The μSR time window can measure magnetic fluctuation rates in the range from 10^4 to 10^{12} Hz [34].

In this Letter, we report a comprehensive μSR investigation of the GS spin dynamics of YbMgGaO₄ using single-crystal samples. Neither the oscillation signal nor characteristic recovery of the polarization to 1/3 is observed in the ZF measurements with the incident μ^+ polarization perpendicular and parallel to the c axis down to 0.048 K and 0.066 K, respectively, thus, ruling out any static uniform or random field exceeding 0.09 mT. The μ^+ spin relaxation rate ($\propto$ Yb^{3+} spin dynamic correlation
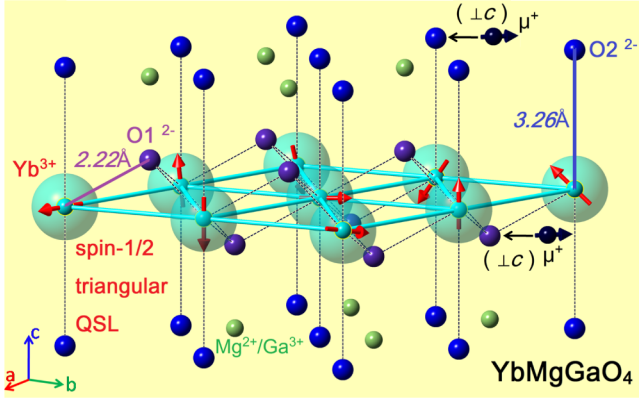
FIG. 1.   Crystal structure of YbMgGaO$_4$ around the effective spin-$\frac{1}{2}$ triangular layer of Yb^{3+}. The implanted μ^+ is likely to stop near O1^{2-} and O2^{2-}, and probes local spin dynamics of the triangular QSL.

FIG. 2.   Selected background-subtracted ZF-μSR signals with the incident beam (a) perpendicular ($\perp$) and (b) parallel ($\parallel$) to the c axis. The colored lines are the corresponding fits to the data using Eq. (1). The insets show relevant experimental geometries.

function) measured in a ZF exhibits a plateau below 0.4 K. These observations strongly suggest that a gapless U(1) QSL GS is formed in YbMgGaO$_4$.

Experimental technique.—Large single crystals (~ 1 cm) of YbMgGaO$_4$ were grown by the floating zone technique [24]. The high quality of the single crystals was confirmed by x-ray diffraction showing narrow reflections with $\Delta(2\theta) \sim 0.04°$ [35]. The crystal orientations were determined by Laue x-ray diffraction. The crystals were cut into slices along both the c axis and the ab plane with a homogeneous thickness of ~ 1 mm. Mosaics of slices along the c axis (S1) and the ab plane (S2) were mounted on two silver sample holders [35]. The μSR data were collected at the ISIS pulsed muon facility, Rutherford Appleton Laboratory, United Kingdom, on both samples (S1 and S2) between 0.05 and 4 K using dilution refrigerators. Additional data between 2 and 50 K were collected by transferring the sample to a ^{4}He cryostat [36]. The international system of units is used throughout this Letter, and $\langle\rangle$ represents thermal and sample average.

Absence of spin freezing.—Implanted muons are very sensitive to local magnetic fields induced by the neighboring Yb^{3+} spins (Fig. 1) [35]. Therefore, ZF-μSR is the best tool to detect long-range magnetic order or spin freezing.

Our ZF and longitudinal-field (LF) data (Figs. 2 and 3) are well fitted to a stretched exponential relaxation function

$$A^{\text{ZF/LF}} = A_0 \exp[-(\lambda t)^\beta] + B_{\text{ZF/LF}}. \quad (1)$$

Here, $A_0 \sim 0.2$ is the initial asymmetry (weakly temperature and field dependent), λ is the μ^+ spin relaxation rate, and β is the stretching exponent. The coefficient $B_{\text{ZF/LF}} \sim 0.13$ is a background constant representing muons that missed the sample. As background constants depend on the sample environment (cryostat), we use background-subtracted ZF/LF data, whereas raw data can be found in the Supplemental Material [35]. For the sample S1, the
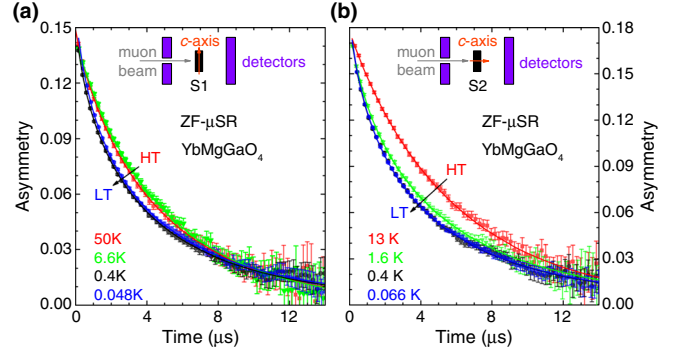
ZF signal increases (by < 0.01) in the critical or crossover temperature range (0.4 to 4 K) at long times, but this effect is within the error bar of the data [35].

The absence of spin freezing in YbMgGaO$_4$ is supported by the following observations. (1) The ZF signals decrease continuously (see Fig. 2) without showing oscillations within the analyzed time window up to 20 μs. This continuous decrease is observed at all temperatures down to 0.048 and 0.066 K with the incident μ^+ polarization perpendicular and parallel to the c axis, respectively [35], suggesting that no static uniform local field is formed. (2) The ZF spectra also lack a recovery of the polarization to 1/3, suggesting the absence of static random fields (no spin-glass-like freezing) [37,38]. (3) The stretching exponent β gradually decreases from ~ 1 at high temperatures ($T \geq 4$ K $\gg J_0$) down to a constant value of ~ 0.6 at the lowest temperatures ($T \sim 0.1$ K $\ll J_0$), see Fig. 4(b). In contrast, for a spin glass system, β is expected to drop to 1/3 at the spin freezing temperature [39,40]. (4) The ZF μ^+ spin relaxation rate λ^{ZF} increases by 50% upon cooling from $T \gg J_0$ ($\lambda^{\text{ZF}} \sim 0.2$ μs^{-1}) down to $T \ll J_0$ ($\lambda^{\text{ZF}} \sim 0.3$ μs^{-1}), see Fig. 2 and Fig. 5. This indicates only a
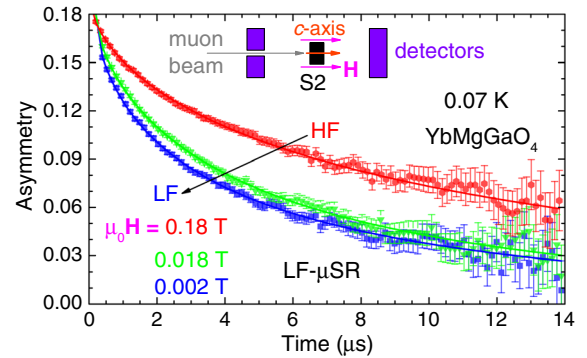

FIG. 3.   Selected LF-μSR signals (background-subtracted) at 0.07 K. The colored lines are fits to the data using Eq. (1). The insets show the experimental geometries.
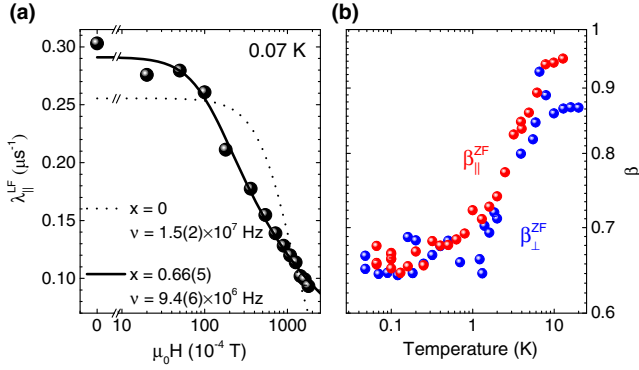
FIG. 4. (a) LF dependence of the μ^+ spin relaxation rate, $\lambda_\parallel^{\mathrm{LF}}(H)$, at 0.07 K. The dotted line represents the fit to the $\lambda_\parallel^{\mathrm{LF}}$ using Eq. (2) ($x = 0$), and the solid line is the fit using Eq. (3) with $x = 0.66(5)$. (b) Temperature dependence of the stretching exponents, β.
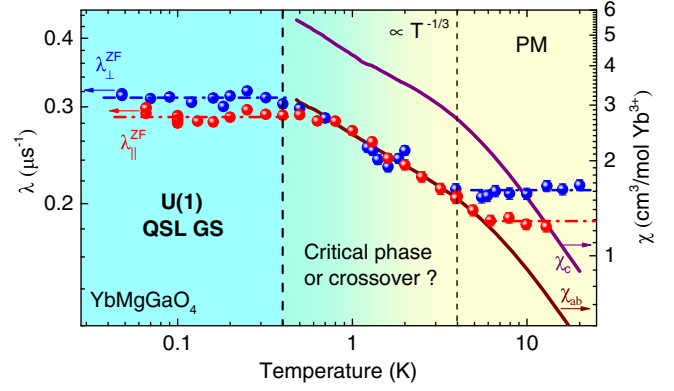

FIG. 5. Temperature dependence of the μ^+ spin relaxation rates from the zero field measurements and from the bulk static susceptibilities measured in the applied field of 0.01 T. PM represents the conventional paramagnetic phase.

weak slowing down of the Yb^{3+} spin fluctuations [41–43], whereas in a spin glass, the relaxation rate will typically increase by several orders of magnitude below the freezing point ($\lambda \sim 1$–$20\ \mu s^{-1}$) [37,38,43]. (5) The LF spectra measured at 0.07 K change gradually and only moderately when the field is increased from 0 to 0.18 T, see Fig. 3 and Fig. 4(a). This is another evidence for the dynamic relaxation and the absence of long range magnetic order down to the lowest temperature.

The upper limit of local static uniform or random fields can be estimated as $(\langle B_{\mathrm{loc}}^{ab}\rangle + \langle B_{\mathrm{loc}}^{c}\rangle)/2 < 0.09$ mT down to 0.048 K and $\langle B_{\mathrm{loc}}^{ab}\rangle < 0.09$ mT down to 0.066 K [35].

Dynamic spin correlation.—At high temperatures ($T > 4$ K), the μ^+ spin relaxations (Fig. 2) can be well fitted by Eq. (1) with a stretching exponent $\beta \sim 1$, indicating a concentrated spin system (spin-1/2 triangular lattice of Yb^{3+}) with very fast spin fluctuations [37,38]. In this case, a Gaussian distribution of local magnetic fields is expected with the width $\Delta \sim \gamma_\mu \sqrt{\langle B_{\mathrm{loc}}^2\rangle}$ and $\langle B_{\mathrm{loc}}\rangle \sim 0$, here $\gamma_\mu = 135.5$ MHz/T is the μ^+ gyromagnetic ratio. In the high-T (mean-field) limit, the Yb^{3+} spin fluctuation rate can be estimated as $\upsilon = \sqrt{z}J_0 s/h \sim 4 \times 10^{10}$ Hz [38], where $z = 6$ is the coordination number.

Above 4 K, μ^+ spin relaxation rates, both $\lambda_\parallel^{\mathrm{ZF}}$ and $\lambda_\perp^{\mathrm{ZF}}$ with the incident μ^+ polarization parallel and perpendicular to the c axis, reach temperature-independent values of $0.185(2)$ and $0.211(1)\ \mu s^{-1}$, respectively (see Fig. 5). Using Eq. (2) with $H = 0$

$$\lambda(T > 4\mathrm{K}, H) = \frac{2\Delta^2\upsilon}{\upsilon^2 + (\mu_0 H\gamma_\mu)^2}, \quad (2)$$

we can estimate the distribution width of the local magnetic fields, $\Delta \sim 6 \times 10^7$ Hz $\ll \upsilon$, confirming the fast spin fluctuation limit [38,43]. The slight difference between $\lambda_\parallel^{\mathrm{ZF}}$ and $\lambda_\perp^{\mathrm{ZF}}$, as well as between $\beta_\parallel^{\mathrm{ZF}}$ and $\beta_\perp^{\mathrm{ZF}}$, is probably rooted in the anisotropic magnetic couplings due to the strong

spin-orbit couplings in Yb^{3+}. At high temperatures, $(2/\upsilon_{ab})/(1/\upsilon_{ab} + 1/\upsilon_c) \sim 2J_{zz}/(J_{zz} + 2J_\pm)$ [24] ~ 0.7 is qualitatively consistent with the measured $\lambda_\parallel^{\mathrm{ZF}}/\lambda_\perp^{\mathrm{ZF}} \sim 0.87$, assuming the isotropic nature of Δ^2 (i.e., $\Delta_c^2 \sim \Delta_{ab}^2$) ($\Delta^2$ should also be anisotropic). Note, also, that $S1$ and $S2$ are different crystals and not two different orientations of the same crystals. Therefore, some sample-related difference in the μSR signal cannot be excluded.

At the lowest temperature of our measurement, $T \sim 0.07$ K, $\lambda_\parallel^{\mathrm{LF}}(H)$ does not follow Eq. (2) [see Fig. 4(a)], suggesting that the spin dynamic autocorrelation function $S(t)$ should take a general form, $S(t) \sim (\tau/t)^x \exp(-\upsilon t)$, instead of the simple exponential form ($x = 0$) [41,42,44], where τ and $1/\upsilon$ are the early and late time cutoffs, respectively, and x can be defined as a critical exponent [45].

A more general expression for the μ^+ spin relaxation rate can be obtained from both semi-classical [42] and full quantum [46] treatments,

$$\lambda(H) = 2\Delta^2\tau^x \int_0^\infty t^{-x}\exp(-\upsilon t)\cos(2\pi\mu_0\gamma_\mu Ht)dt. \quad (3)$$

For a spin system at $T \gg J_0$, the μ^+ relaxation rates take the simple form of Eq. (2). On the other hand, at 0.07 K, $\lambda_\parallel^{\mathrm{LF}}(H)$ is much better described by Eq. (3) with $x = 0.66(5)$ and $\upsilon = 9.4(6) \times 10^6$ Hz [see Fig. 4(a)]. This way, at low temperatures, $S(t)$ behaves more power-law-like and attenuates much slower than $S(t) \sim \exp(-\upsilon t)$ with $\upsilon \sim 4 \times 10^{10}$ Hz at high temperatures [35,42]. It suggests the onset of long-time spin correlations at low temperatures. The Yb^{3+} spins in $YbMgGaO_4$ are strongly entangled not only in space, but also in time, yet without showing symmetry breaking or spin freezing, thus, meeting the basic requirements of a gapless quantum spin liquid.

All of the fitted stretching exponents β gradually decrease as the temperature goes down. At $T < 0.4$ K, the stretching exponent β approaches a constant value of

~0.6, indicating a distribution of the μ^+ spin relaxation rates [see Fig. 4(b)]. This decrease is a very common phenomenon in lots of frustrated magnets and may be caused by the onset of Yb^{3+} spin correlations in space [47].

Muon spin relaxation rate.—Spin relaxation rates λ provide further insight into the GS spin dynamics of the system, because a dynamic local magnetic field is induced by the effective spin-$1/2$ moment of Yb^{3+} on the triangular lattice. The ZF-μ^+ spin relaxation rate can be expressed as [41–43]

$$\lambda^{ZF} = \gamma_\mu^2 \int_0^\infty \langle \mathbf{B}_{loc}^\perp(t) \cdot \mathbf{B}_{loc}^\perp(0) \rangle dt \propto S_{\omega \to 0}^\perp, \quad (4)$$

where $S_{\omega \to 0}^\perp = \int_0^\infty \langle \mathbf{s}_i^\perp(t) \cdot \mathbf{s}_i^\perp(0) \rangle dt$ is the static spin structure factor with the sum over $\mathbf{q}$ [48].

As the temperature goes down, all of the μ^+ spin relaxation rates gradually increase by about 50% compared to the high-T limit and get saturated below 0.4 K (see Fig. 5). These observations indicate the slowing down of spin fluctuations.

Phase diagram and conclusions.—Our observations indicate that strong phase-coherent quantum fluctuations of Yb^{3+} spins survive at low temperatures. Upon changing the temperature from above 4 K to below 0.4 K and suppressing the energy of thermal fluctuations by at least 1 order of magnitude, about 2/3 of the total fluctuations at $T > 4$ K are retained due to the strong geometrical frustration [1]. The spin relaxation rate λ^{ZF} saturates below $T_s \simeq 0.4$ K (Fig. 5). This characteristic temperature of 0.4 K is nearly the same as in other QSL candidates [44,47,49–51] but is significantly higher on the relative energy scale of $YbMgGaO_4$ ($T_s/J_0 \sim 0.27$). We suggest that quantum fluctuations have a paramount effect below this temperature, regardless of the absolute scale of the magnetic couplings J_0.

Several distinct regimes of $YbMgGaO_4$ can also be inferred from the temperature evolution of the bulk static susceptibility and μ^+ spin relaxation rates, as shown in Fig. 5. At $T > 4$ K, the susceptibilities follow the Curie-Weiss law [24], and the μ^+ spin relaxation rates are constants, as is typical for the paramagnetic regime [38,41,47,49–51]. The spins are still short-time correlated with $S(t) \sim \exp(-vt)$. This high-temperature phase is compatible with the classical paramagnet. As the temperature goes down (0.4 K $< T <$ 4 K), the spin susceptibilities show an unconventional critical behavior $\chi \sim T^{-1/3}$, and the μ^+ spin relaxation rates increase by 50% following the uniform spin susceptibilities (Fig. 5).

At even lower temperatures ($T < 0.4$ K), the μ^+ spin relaxation rates approach constant values again (Fig. 5). This behavior appears to be generic for frustrated magnets [38,41,47,49–51]. The temperature-independent μ^+ spin relaxation rates suggest a constant spin correlation $S_{\omega \to 0}$ with the sum over $\mathbf{q}$, which is consistent with the triangular U(1) QSL GS [18–20].

In conclusion, we performed a comprehensive study of spin dynamics in the frustrated antiferromagnet $YbMgGaO_4$ by μSR measurements using the high-quality single crystals along both the c axis and the ab plane. No static uniform or random field is detected ($\langle B_{loc} \rangle < 0.09$ mT), indicating the absence of spin freezing ($\langle \mathbf{s}_j \rangle \sim 0$) down to at least 0.048 K. The spin correlation function reaches a constant value below 0.4 K. Long-time Yb^{3+} spin correlations are developed in this temperature range. Combined with the heat-capacity data [23], our observations provide compelling evidence for the formation of gapless U(1) QSL GS in the triangular antiferromagnet $YbMgGaO_4$.

The concept of the U(1) QSL has been applied to a gamut of systems, from spin-ice pyrochlores [52,53] to high-temperature superconductors [54], but experimental observation of this state remains elusive. Spin liquids in the organic charge-transfer salts with the frustrated triangular geometry deviate from the anticipated U(1) behavior [18,21,22]. In contrast, $YbMgGaO_4$ displays several phenomenological signatures of this state: (i) the absence of long-range magnetic order and spin freezing, (ii) the constant magnetic susceptibility at low temperatures, (iii) the $C_v \simeq T^{2/3}$ power-law behavior of the specific heat [23]. Our findings pave the way for observing further emergent properties of the triangular U(1) QSL, including the $\kappa \simeq T^{1/3}$ behavior of thermal conductivity and violation of the Wiedemann-Franz law [19,55], the power-law optical conductivity inside the Mott gap [56], and surface plasmons driven by spinons [57]. Exact origin of the U(1) QSL GS of $YbMgGaO_4$ is also of interest. In contrast to the organic charge-transfer salts, where long-range magnetic order is destabilized by ring exchange, spin-orbit coupling and the ensuing magnetic anisotropy are the most likely effects that trigger strong frustration in this material [58].

*yuesheng.man.li@gmail.com
†qmzhang@ruc.edu.cn

[1] L. Balents, Spin liquids in frustrated magnets, Nature (London) **464**, 199 (2010).

[2] P. A. Lee, An end to the drought of quantum spin liquids, Science **321**, 1306 (2008).

[3] X.-G. Wen, *Quantum Field Theory of Many-Body Systems: From the Origin of Sound to an Origin of Light and Electrons* (Oxford University Press, New York, 2004).

[4] P. W. Anderson, Resonating valence bonds: A new kind of insulator?, Mater. Res. Bull. **8**, 153 (1973).

[5] P. W. Anderson, The resonating valence bond state in La_2CuO_4 and superconductivity, Science **235**, 1196 (1987).

[6] G. Baskaran, Z. Zou, and P. W. Anderson, The resonating valence bond state and high-t_c superconductivity: A mean field theory, Solid State Commun. **63**, 973 (1987).

[7] R. R. P. Singh and D. A. Huse, Three-Sublattice Order in Triangular- and Kagomé-Lattice Spin-Half Antiferromagnets, Phys. Rev. Lett. **68**, 1766 (1992).

[8] P. Sindzingre, P. Lecheminant, and C. Lhuillier, Investigation of different classes of variational functions for the triangular and kagomé spin-1/2 Heisenberg antiferromagnets, Phys. Rev. B **50**, 3108 (1994).

[9] B. Bernu, P. Lecheminant, C. Lhuillier, and L. Pierre, Exact spectra, spin susceptibilities, and order parameter of the quantum Heisenberg antiferromagnet on the triangular lattice, Phys. Rev. B **50**, 10048 (1994).

[10] L. Capriotti, A. E. Trumper, and S. Sorella, Long-Range Néel Order in the Triangular Heisenberg Model, Phys. Rev. Lett. **82**, 3899 (1999).

[11] Z. Weihong, R. H. McKenzie, and R. P. Singh, Phase diagram for a class of spin-$\frac{1}{2}$ Heisenberg models interpolating between the square-lattice, the triangular-lattice, and the linear-chain limits, Phys. Rev. B **59**, 14367 (1999).

[12] R. Kaneko, S. Morita, and M. Imada, Gapless spin-liquid phase in an extended spin-$\frac{1}{2}$ triangular Heisenberg model, J. Phys. Soc. Jpn. **83**, 093707 (2014).

[13] P. H. Y. Li, R. F. Bishop, and C. E. Campbell, Quasiclassical magnetic order and its loss in a spin-$\frac{1}{2}$ Heisenberg antiferromagnet on a triangular lattice with competing bonds, Phys. Rev. B **91**, 014426 (2015).

[14] A. E. Trumper, Spin-wave analysis to the spatially anisotropic Heisenberg antiferromagnet on a triangular lattice, Phys. Rev. B **60**, 2987 (1999).

[15] S. Yunoki and S. Sorella, Two spin liquid phases in the spatially anisotropic triangular Heisenberg model, Phys. Rev. B **74**, 014408 (2006).

[16] T. Ohashi, T. Momoi, H. Tsunetsugu, and N. Kawakami, Finite Temperature Mott Transition in Hubbard Model on Anisotropic Triangular Lattice, Phys. Rev. Lett. **100**, 076402 (2008).

[17] K. Watanabe, H. Kawamura, H. Nakano, and T. Sakai, Quantum spin-liquid behavior in the spin-1/2 random Heisenberg antiferromagnet on the triangular lattice, J. Phys. Soc. Jpn. **83**, 034714 (2014).

[18] O. I. Motrunich, Variational study of triangular lattice spin-$\frac{1}{2}$ model with ring exchanges and spin liquid state in κ-$(ET)_2Cu_2(CN)_3$, Phys. Rev. B **72**, 045105 (2005).

[19] S.-S. Lee and P. A. Lee, U(1) Gauge Theory of the Hubbard Model: Spin Liquid States and Possible Application to κ-$(BEDT\text{-}TTF)_2Cu_2(CN)_3$, Phys. Rev. Lett. **95**, 036403 (2005).

[20] O. I. Motrunich, Orbital magnetic field effects in spin liquid with spinon Fermi sea: Possible application to κ-$(ET)_2Cu_2(CN)_3$, Phys. Rev. B **73**, 155115 (2006).

[21] S. Yamashita, Y. Nakazawa, M. Oguni, Y. Oshima, H. Nojiri, Y. Shimizu, K. Miyagawa, and K. Kanoda, Thermodynamic properties of a spin-1/2 spin-liquid state in a κ-type organic salt, Nat. Phys. **4**, 459 (2008).

[22] S. Yamashita, T. Yamamoto, Y. Nakazawa, M. Tamura, and R. Kato, Gapless spin liquid of an organic triangular compound evidenced by thermodynamic measurements, Nat. Commun. **2**, 275 (2011).

[23] Y. Li, H. Liao, Z. Zhang, S. Li, F. Jin, L. Ling, L. Zhang, Y. Zou, L. Pi, Z. Yang *et al.*, Gapless quantum spin liquid ground state in the two-dimensional spin-1/2 triangular antiferromagnet YbMgGaO$_4$, Sci. Rep. **5**, 16419 (2015).

[24] Y. Li, G. Chen, W. Tong, L. Pi, J. Liu, Z. Yang, X. Wang, and Q. Zhang, Rare-Earth Triangular Lattice Spin Liquid: A Single-Crystal Study of YbMgGaO$_4$, Phys. Rev. Lett. **115**, 167203 (2015).

[25] S.-H. Lee, H. Kikuchi, Y. Qiu, B. Lake, Q. Huang, K. Habicht, and K. Kiefer, Quantum-spin-liquid states in the two-dimensional kagome antiferromagnets $Zn_xCu_{4-x}(OD)_6Cl_2$, Nat. Mater. **6**, 853 (2007).

[26] D. E. Freedman, T. H. Han, A. Prodi, P. Müller, Q.-Z. Huang, Y.-S. Chen, S. M. Webb, Y. S. Lee, T. M. McQueen, and D. G. Nocera, Site specific x-ray anomalous dispersion of the geometrically frustrated kagome magnet, herbertsmithite, $ZnCu_3(OH)_6Cl_2$, J. Am. Chem. Soc. **132**, 16185 (2010).

[27] Y. Li and Q. Zhang, Structure and magnetism of $s = \frac{1}{2}$ kagome antiferromagnets $NiCu_3(OH)_6Cl_2$ and $CoCu_3(OH)_6Cl_2$, J. Phys. Condens. Matter **25**, 026003 (2013).

[28] Y. Li, J. Fu, Z. Wu, and Q. Zhang, Transition-metal distribution in kagome antiferromagnet $CoCu_3(OH)_6Cl_2$ revealed by resonant x-ray diffraction, Chem. Phys. Lett. **570**, 37 (2013).

[29] Y. Li, B. Pan, S. Li, W. Tong, L. Ling, Z. Yang, J. Wang, Z. Chen, Z. Wu, and Q. Zhang, Gapless quantum spin liquid in the $s = 1/2$ anisotropic kagome antiferromagnet $ZnCu_3(OH)_6SO_4$, New J. Phys. **16**, 093011 (2014).

[30] Y. Shimizu, K. Miyagawa, K. Kanoda, M. Maesato, and G. Saito, Spin Liquid State in an Organic Mott Insulator with a Triangular Lattice, Phys. Rev. Lett. **91**, 107001 (2003).

[31] T. Itou, A. Oyamada, S. Maegawa, M. Tamura, and R. Kato, Quantum spin liquid in the spin-1/2 triangular antiferromagnet $EtMe_3Sb[Pd(dmit)_2]_2$, Phys. Rev. B **77**, 104413 (2008).

[32] T. Moriya, New Mechanism of Anisotropic Superexchange Interaction, Phys. Rev. Lett. **4**, 228 (1960).

[33] A. Zorko, S. Nellutla, J. Van Tol, L. C. Brunel, F. Bert, F. Duc, J.-C. Trombe, M. A. De Vries, A. Harrison, and P. Mendels, Dzyaloshinsky-Moriya Anisotropy in the Spin-1/2 Kagome Compound $ZnCu_3(OH)_6Cl_2$, Phys. Rev. Lett. **101**, 026405 (2008).

[34] S. J. Blundell, Spin-polarized muons in condensed matter physics, Contemp. Phys. **40**, 175 (1999).

[35] See Supplemental Material at http://link.aps.org/supplemental/10.1103/PhysRevLett.117.097201 for detailed information about experimental procedures.

[36] A. D. Hillier, P. J. C. King, S. P. Cottrell, and J. S. Lord, *The MuSR User Guide* (ISIS Facility, STFC, Rutherford Appleton Laboratory, Oxford, England, 2005).

[37] Y. J. Uemura, T. Yamazaki, D. R. Harshman, M. Senba, and E. J. Ansaldo, Muon-spin relaxation in AuFe and CuMn spin glasses, Phys. Rev. B **31**, 546 (1985).

[38] Y. J. Uemura, A. Keren, K. Kojima, L. P. Le, G. M. Luke, W. D. Wu, Y. Ajiro, T. Asano, Y. Kuriyama, M. Mekata *et al.*, Spin Fluctuations in Frustrated Kagomé Lattice System $SrCr_8Ga_4O_{19}$ Studied by Muon Spin Relaxation, Phys. Rev. Lett. **73**, 3306 (1994).

[39] A. T. Ogielski, Dynamics of three-dimensional Ising spin glasses in thermal equilibrium, Phys. Rev. B **32**, 7384 (1985).

[40] I. A. Campbell, A. Amato, F. N. Gygax, D. Herlach, A. Schenck, R. Cywinski, and S. H. Kilcoyne, Dynamics in Canonical Spin Glasses Observed by Muon Spin D depolarization, Phys. Rev. Lett. **72**, 1291 (1994).

[41] A. Keren, J. S. Gardner, G. Ehlers, A. Fukaya, E. Segal, and Y. J. Uemura, Dynamic Properties of a Diluted Pyrochlore Cooperative Paramagnet $(Tb_pY_{1-p})_2Ti_2O_7$, Phys. Rev. Lett. **92**, 107204 (2004).

[42] A. Keren, G. Bazalitsky, I. Campbell, and J. S. Lord, Probing exotic spin correlations by muon spin depolarization measurements with applications to spin glass dynamics, Phys. Rev. B **64**, 054403 (2001).

[43] D. Bono, P. Mendels, G. Collin, N. Blanchard, F. Bert, A. Amato, C. Baines, and A. D. Hillier, μSR Study of the Quantum Dynamics in the Frustrated $s = \frac{3}{2}$ Kagomé Bilayers, Phys. Rev. Lett. **93**, 187201 (2004).

[44] E. Kermarrec, P. Mendels, F. Bert, R. H. Colman, A. S. Wills, P. Strobel, P. Bonville, A. Hillier, and A. Amato, Spin-liquid ground state in the frustrated kagome antiferromagnet $MgCu_3(OH)_6Cl_2$, Phys. Rev. B **84**, 100401 (2011).

[45] P. C. Hohenberg and B. I. Halperin, Theory of dynamic critical phenomena, Rev. Mod. Phys. **49**, 435 (1977).

[46] T. McMullen and E. Zaremba, Positive-muon spin depolarization in solids, Phys. Rev. B **18**, 3026 (1978).

[47] L. Clark, J. C. Orain, F. Bert, M. A. De Vries, F. H. Aidoudi, R. E. Morris, P. Lightfoot, J. S. Lord, M. T. F. Telling, P. Bonville *et al.*, Gapless Spin Liquid Ground State in the $s = \frac{1}{2}$ Vanadium Oxyfluoride Kagome Antiferromagnet $[NH_4]_2[\tilde{C}_7H_{14}N][V_7O_6F_{18}]$, Phys. Rev. Lett. **110**, 207208 (2013).

[48] A. Avella and F. Mancini, *Strongly Correlated Systems: Numerical Methods* (Springer, Berlin, 2013), Vol. 176.

[49] B. Fåk, E. Kermarrec, L. Messio, B. Bernu, C. Lhuillier, F. Bert, P. Mendels, B. Koteswararao, F. Bouquet, J. Ollivier *et al.*, Kapellasite: A Kagome Quantum Spin Liquid with Competing Interactions, Phys. Rev. Lett. **109**, 037208 (2012).

[50] M. Gomilsek, M. Klanjsek, M. Pregelj, H. Luetkens, Y. Li, Q. M. Zhang, and A. Zorko, μSR insight into the impurity problem in quantum kagome antiferromagnets, Phys. Rev. B **94**, 024438 (2016).

[51] M. Gomilšek, M. Klanjšek, M. Pregelj, F. C. Coomer, H. Luetkens, O. Zaharko, T. Fennell, Y. Li, Q. M. Zhang, and A. Zorko, Instabilities of spin-liquid states in a quantum kagome antiferromagnet, Phys. Rev. B **93**, 060405 (2016).

[52] M. Hermele, M. P. A. Fisher, and L. Balents, Pyrochlore photons: The $U(1)$ spin liquid in a $s = \frac{1}{2}$ three-dimensional frustrated magnet, Phys. Rev. B **69**, 064404 (2004).

[53] L. Savary and L. Balents, Coulombic Quantum Liquids in Spin-1/2 Pyrochlores, Phys. Rev. Lett. **108**, 037202 (2012).

[54] P. A. Lee, From high temperature superconductivity to quantum spin liquid: progress in strong correlation physics, Rep. Prog. Phys. **71**, 012501 (2008).

[55] C. P. Nave and P. A. Lee, Transport properties of a spinon Fermi surface coupled to a $U(1)$ gauge field, Phys. Rev. B **76**, 235124 (2007).

[56] T.-K. Ng and P. A. Lee, Power-Law Conductivity inside the Mott Gap: Application to κ-$(BEDT-TTF)_2Cu_2(CN)_3$, Phys. Rev. Lett. **99**, 156402 (2007).

[57] Y.-F. Ma and T.-K. Ng, Surface plasmons and reflectance of $U(1)$ spin liquid states with large spinon Fermi surfaces, Phys. Rev. B **91**, 075106 (2015).

[58] Y. D. Li, X. Wang, and G. Chen, Anisotropic spin model of strong spin-orbit-coupled triangular antiferromagnets, Phys. Rev. B **94**, 035107 (2016).